Probing the Mechanism of Incorporation of Fluorescently Labeled Actin into Stress Fibers

Philip A. Amato and D. Lansing Taylor

Department of Biological Sciences and Center for Fluorescence Research in Biomedical Sciences, Carnegie-Mellon University, Pittsburgh, Pennsylvania 15213. Dr. Amato's present address is Photonic Microscopy, Inc., 2625 Butterfield Road, Suite 204S, Oak Brook, Illinois 60521.

Abstract. The mechanism of actin incorporation into and association with stress fibers of 3T3 and WI38 fibroblasts was examined by fluorescent analog cytochemistry, fluorescence recovery after photobleaching (FRAP), image analysis, and immunoelectron microscopy. Microinjected, fluorescein-labeled actin (AF-actin) became associated with stress fibers as early as 5 min post-injection. There was no detectable cellular polarity in the association of AF-actin with pre-existing stress fibers relative to perinuclear or peripheral regions. The rate of incorporation was quantified by image analysis of images generated with a two-dimensional photon counting microchannel plate camera. After equilibration of up to 2 h post-injection, FRAP demonstrated that actin subunits exchanged rapidly between filaments in stress fibers and the surrounding cytoplasm. When co-injected with rhodamine-labeled bovine serum albumin as a control, only actin was detected in the phase-dense stress fibers. The control protein was excluded from fibers and any linear fluorescence of the control was demonstrated as a path-length artifact. The incorporation of AF-actin into stress fibers was studied by immunoelectron microscopy using anti-fluorescein as the primary antibody and goat anti-rabbit IgG coupled to peroxidase as the secondary antibody. At 5 min post-injection, reaction product was localized periodically in some fibers with a periodicity of ~0.75 μm. In large diameter fibers at 5 min post-injection, the analog was seen first on the surface of fibers, with individual filaments resolvable within the core. In the same cell, thinner diameter fibers were labeled uniformly throughout the diameter. By 20 min post-injection, most fibers were uniformly labeled. We conclude that the rate of actin subunit exchange in vivo is extremely rapid with molecular incorporation into actin filaments of stress fibers occurring as early as a few minutes post-injection. Exchange appears to first occur in filaments along the surface of stress fibers and then into more central regions in a periodic manner. We suggest that the periodic localization of actin at very early time points is due to a local microheterogeneity in which microdomains of fast vs. slower incorporation result from the periodic localization of actin-binding protein, such as α-actinin, along the length of the fiber.

STRESS fibers in fibroblasts are dense parallel arrays of actin filaments containing a large number of actin-binding proteins. Several interesting and unique isolation procedures have helped to describe their biochemical constituents (22, 27). In addition, the structural organization of stress fibers has been defined, primarily by electron microscopy (2, 5, 11, 20) and by immunofluorescence (3, 14, 18).

A sarcomeric-like distribution of contractile proteins has been demonstrated in certain classes of stress fibers (6, 19, 21). Immunofluorescence studies have shown that myosin and tropomyosin are both localized in a discontinuous pattern which is anti-periodic to the distribution of α-actinin (12, 13, 21, 32). In addition, cell models have demonstrated that stress fibers are capable of contracting (7, 8). It is not presently known, however, whether the sarcomeric structure or contractility of stress fibers plays a basic role in fibroblast movement.

Fluorescent analog cytochemistry has permitted the study of the dynamics of specific cytoskeletal components in stress fibers of living cells (for reviews see references 23, 29). The microinjection of fluorescent analogs of actin into fibroblasts results in the formation of distinct fluorescent fibers suggesting that the analog is actively incorporated into endogenous actin filaments (4, 9, 10, 33). The rapid rate of apparent actin analog incorporation was noted early (4). Fluorescence recovery after photobleaching (FRAP)[1] measurements of actin in stress fibers also suggests that actin subunits are readily exchanged (10). Finally, the study of actin analogs in stress fibers has shown that stress fibers are capable of rapid reorganization

[1] *Abbreviations used in this paper:* AF-actin, fluorescein-labeled actin; FRAP, fluorescence recovery after photobleaching.

during cell movement and in response to various stimuli (24, 28).

This study addresses two related questions: (*a*) do fluorescent analogs of actin incorporate into the actin filaments within stress fibers at the molecular level, and (*b*) if so, are there preferred domains of incorporation relative to the cell center or along the length of fibers? On the basis of our findings, we suggest that the structural and regulatory components of stress fibers in vivo can inhibit or promote the incorporation of microinjected, fluorescein-labeled actin (AF-actin).

Materials and Methods

Cell Culture

Swiss albino mouse 3T3 fibroblasts were grown at 37°C in Dulbecco's modified Eagle's medium (Gibco Laboratories, Grand Island, NY.) supplemented with 10% calf serum (Gibco). Human lung WI38 fibroblasts were grown in modified Eagle's medium with Earle's balanced salt solution (Gibco) supplemented with 10% fetal calf serum (Gibco). Both cell lines were obtained from American Type Culture Collection, Rockville, MD. Cells were trypsinized and plated on Gold Seal microscope slides (Fisher Scientific Co., Pittsburgh, PA) at a density of ~1 × 10^5 cells/cm 24 h before microinjection.

Preparation of Labeled Proteins

Actin, prepared from rabbit back and leg muscles, and bovine serum albumin (BSA) (Worthington Biochemical Corp., Freehold, NJ or Sigma Chemical Co., St. Louis, MO) were labeled with 5-iodoacetamido-fluorescein and lissamine rhodamine B sulfonyl chloride, respectively. The details of the labeling and storage procedure are described well elsewhere (31). Fluorescent actin was microinjected in the G-form at a concentration of 3–4 mg/ml; BSA was microinjected at a similar concentration. The dye-to-protein ratio of labeled actin was 0.7–0.9; the dye-to-protein ratio of labeled BSA was 1.0–2.5. For co-injection, the concentrations of the proteins were adjusted so that the two fluorophores were present in equimolar concentrations (16).

Microinjection and Cell Models

The details of the microinjection procedure are described elsewhere (1, 16). The injection volume ranged from ~2.0–10.0% of the total cell volume. Therefore, the final concentration of labeled, monomeric actin perturbing the cell ranged from ~0.06–0.4 mg/ml. No major differences were detected from cell to cell based on the final concentration of actin analog.

For the time course experiments, a number of cells within a small area were microinjected within a few minutes and then recorded. The location of the microinjected cells was easily determined by scribing a circle on the bottom of the glass slide prior to microinjection. For immunocytochemical experiments, slides were either immediately fixed after microinjection or placed in plastic Petri dishes containing complete bicarbonate-buffered culture media and incubated at 37°C in a CO_2 incubator for various time points. After incubation, slides were similarly fixed and processed for immunofluorescence or immunoelectron microscopy.

For some experiments, microinjected cells were extracted with 0.05% Triton X-100 in PBS for 1 min, followed by fixation in 3.7% formaldehyde-0.05% Triton X-100 in PBS for 10 min at room temperature. Cells were then photographed as described below.

Cell models were prepared in which fluorescent filamentous actin was "templated" onto existing stress fibers in fixed and extracted cells. These cell models were used as a control for actin incorporation. Plated cells were permeabilized and lightly fixed in a 0.05% Triton X-100/3.7% formaldehyde in Ca^{++}, Mg^{++}-free PBS solution for 2 min at 37°C. This was followed by further fixation in 3.7% formaldehyde in PBS for 10 min at 37°C. AF-actin was polymerized in buffer containing 100 mM KCl, 2 mM $MgCl_2$, 0.5 mM ATP, and 1 mM PIPES, pH 7.0, for 15 min at room temperature. Cells were incubated with filamentous AF-actin in this buffer for 5 min at 37°C. After rinsing, cells were post-fixed for 2 min with 3.7% formaldehyde at room temperature. After rinsing, cells were incubated with anti-fluorescein rabbit IgG, followed by either rhodamine-labeled goat anti-rabbit IgG for light microscopic viewing, or with peroxidase-labeled goat anti-rabbit IgG for electron microscopy.

Light Microscopy

Microinjection of cells plated on glass slides was performed on a Zeiss inverted microscope equipped with a 40X phase, oil immersion objective (numerical aperture [NA] = 0.85). After microinjection, fluorescence distribution was recorded on a Zeiss photomicroscope equipped with either a Zeiss/Venus 3-stage intensified camera, a DAGE/MTI intensified SIT camera, or a Hamamatsu 2-stage microchannel plate camera (MCP) as indicated. The objective used was a 63X Plan Neofluar water immersion objective (NA = 1.2). Phase-contrast images were obtained with a 40X phase, water immersion objective (NA = 0.75). Sequential images of actin distribution in the same cell were obtained using low light illumination from a 60-W tungsten lamp. Images were recorded on a NEC ¾″ video cassette recorder, as described previously (26). Selected video images were photographed from the TV monitor also as described previously (16, 26). For some experiments, extracted and fixed cells were photographed directly on the photomicroscope with Ilford HP5 film developed with Diafine developer.

Image Analysis and Fluorescence Recovery after Photobleaching

The Hamamatsu Image Processing System (C1966) was used to analyze the rate of incorporation of labeled actin into stress fibers and to analyze the sites and rate of recovery of fluorescence into stress fibers after photobleaching. The studies on the rate of actin incorporation used the Hamamatsu MCP-camera with the luminous flux of excitation light at the specimen plane equal to 35 $\mu W/cm^2$. Images were integrated for 20 s (600 frames) and then stored on video tape using the NEC ¾″ video cassette recorder which was connected to the processor. Under these conditions, the kinetics of actin incorporation could be determined by analyzing images at different time points after injection. Selected frames from the tape were entered into the frame memory and the intensity values over stress fibers were averaged over a 10 = μm segment of the fiber. Five cells were analyzed.

FRAP was performed essentially as described previously (17). The argon ion laser (Spectra-Physics Inc., Mountain View, CA) was operated at 150 mW with the 488-nm line. The duration of the photobleaching pulses ranged from 2.8 ms to 10.4 ms with a spot size of 6.0 μm radius. Epi-illumination of the whole field using low light level excitation was used to record images with a DAGE/MTI ISIT camera after photobleaching. Images were stored on ¾″ video cassette tape. Subsequently, the video cassette tape recordings were played into the Hamamatsu image processing system and 16 frames were averaged and stored in the frame memory for each time point. The integrated intensity within the bleached region was determined at each time point.

Immunocytochemistry and Electron Microscopy

After microinjection, cells were rinsed in phosphate-buffered saline (PBS) and fixed for 10 min in 0.5% glutaraldehyde in PBS at 37°C. After rinsing with PBS, cells were extracted for 10 min with 0.5% Triton X-100 in PBS at room temperature. Cells were rinsed with PBS and endogenous peroxidase activity was inhibited by incubating slides in 3% H_2O_2 solution for 5 min at room temperature. After rinsing in distilled water and PBS, nonspecific background staining was suppressed by incubating slides in a 1% normal goat serum/4% BSA in PBS solution for 15 min at room temperature. The serum suppressor solution was shaken off and a 1:150 dilution of rabbit anti-fluorescein IgG (a gift of Dr. Katherine Luby-Phelps, Carnegie-Mellon University) was directly applied, and incubated for 20 min at 37°C. After rinsing three times with PBS, slides were incubated with a 1:100 dilution of goat anti-rabbit IgG coupled to horseradish peroxidase (Cappel Laboratories, Cochranville, PA) for 20 min at 37°C. Slides were rinsed twice with PBS and then with Tris-HCl buffer. Slides were then incubated with 0.5 mg/ml 3,3′diaminobenzidine tetrahydrochloride solution (Polysciences, Inc., Warrington, PA) with H_2O_2 for 10 min at room temperature. After rinsing with Tris-HCl buffer and PBS, cells were re-fixed with 1% OsO_4 for 2 min followed by 2% glutaraldehyde for 10 min at room temperature. Cells were then rinsed, dehydrated in graded acetone solutions, infiltrated, and embedded in a thin layer of Epon 812.

The layer of Epon was peeled off the glass slide, removing the embedded cells. Microinjected cells were located in the Epon layer with a dissecting microscope, cut out of the resin, and glued to a block face with epoxy. The cell was then serially sectioned parallel to the plane of the substrate. Thin sections were poststained for 10 min with 1% uranyl acetate and for 2 min with lead citrate. Sections were viewed on a Phillips 300 electron microscope at an accelerating voltage of 60 kV.

Results

The Time Course of AF-Actin Incorporation

AF-actin in the monomeric state was injected alone into 3T3 fibroblasts which had been plated 24 h before injection. For

a given cell, the first image recorded was usually 3–5 min post-injection, and sequential images of the same cell were generally taken at 10–15-min intervals (see figure legends).

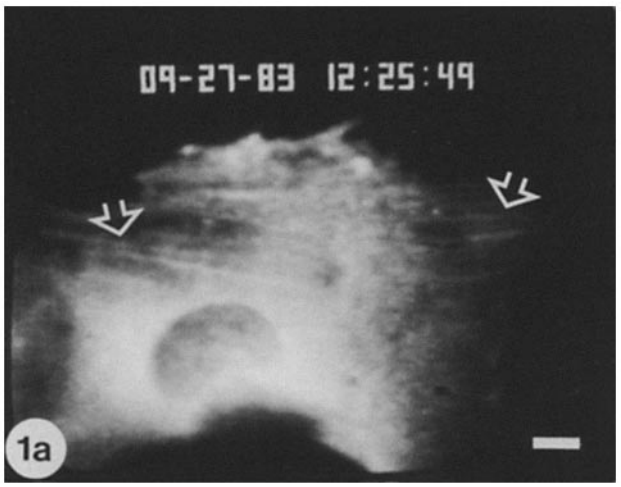

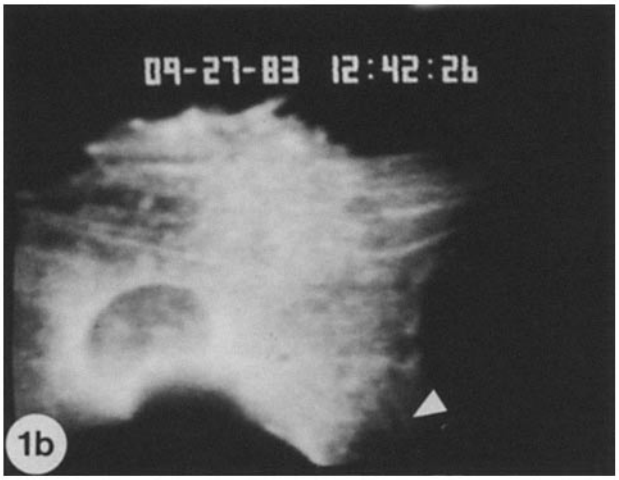

Figure 1. Sequential video images of a 3T3 cell microinjected with AF-actin (*a*) 3–5 min, (*b*) 20 min, and (*c*) 40 min post-injection. AF-actin becomes associated with stress fibers as early as 3–5 min post-injection (*a*, open arrows). In the same cell, these fibers become more distinct and additional fibers can be seen forming *de novo* at later times (*b* and *c*, arrowheads). Note that a newly formed fiber at 40 min post-injection appears discontinuously fluorescent along its length and punctate in several locations (*c*, arrow). Bar, 10 μm.

The distribution of actin fluorescence and the appearance of actin fibers varied from cell to cell depending on such factors as the state of motility and geometric shape of the individual cell. However, actin was qualitatively observed to be incorporated into stress fibers in a large number of cells as early as 5 min post-injection (Fig. 1 *a*). In the same cell, these fibers became more distinct and additional fibers were seen forming in later images (Fig. 1, *b* and *c*). Note that a fiber formed at 40 min post-injection (Fig. 1 *c*, arrow) appears discontinuously fluorescent along its length and punctate in several locations. The appearance of a fiber first as a linear punctate structure and later as a uniformly fluorescent fiber was observed in many cells. Immunofluorescent localization of AF-actin after fixation of microinjected cells using anti-fluorescein and rhodamine-labeled IgG also showed distinct fibers at 5 min post-injection (Fig. 2). The actin distribution of other cells (Fig. 3) changed from nearly completely diffuse immediately after injection (Fig. 3 *a*) to a pattern in which fluorescent fibers were formed at later time points (Fig. 3 *c*).

The first stage of these studies used the Zeiss/Venus 3-stage image intensifier as an analog detector with video tape recording. We improved our estimate of the rate of incorporation of labeled actin into stress fibers by using image analysis of images recorded at ultra-low light levels with the Hamamatsu MCP-camera. Fig. 4 is a plot of the kinetics of actin fluorescence associated with stress fibers after injection. A half-time of incorporation in three separate stress fibers in this same cell ranged from 3.3 to 4 min. Furthermore, at least

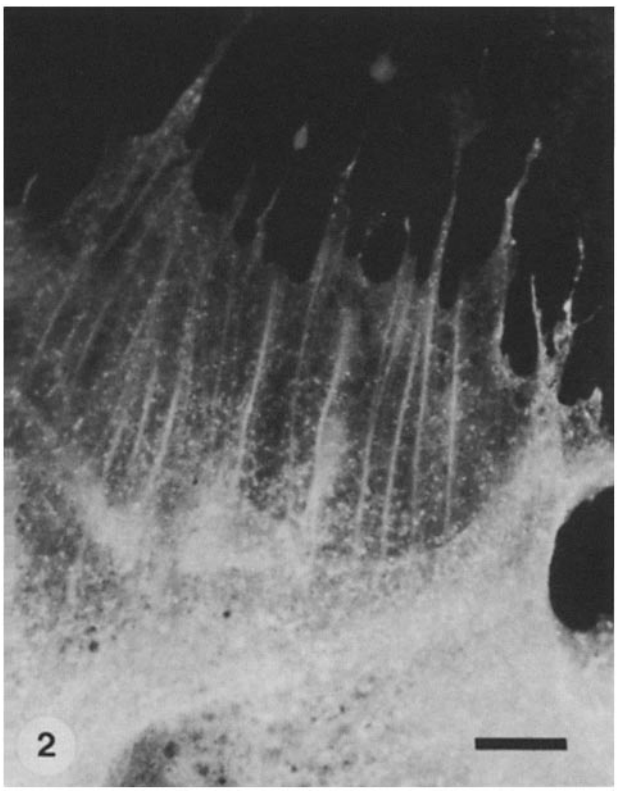

Figure 2. Rhodamine fluorescence of a 3T3 cell, microinjected with AF-actin, fixed at 5 min post-injection, and labeled with anti-fluorescein and rhodamine-labeled IgG. Note the appearance of many fibers at this early time point. The greater visibility of fibers in fixed cells as compared to living cells is probably due to partial extraction of the background soluble pool of actin. Bar, 20 μm.

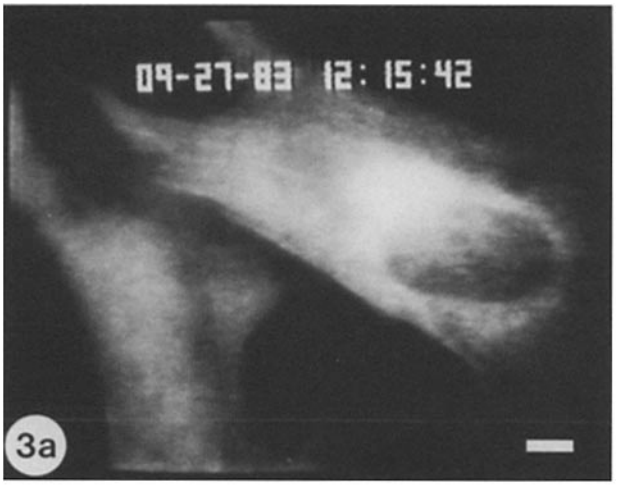

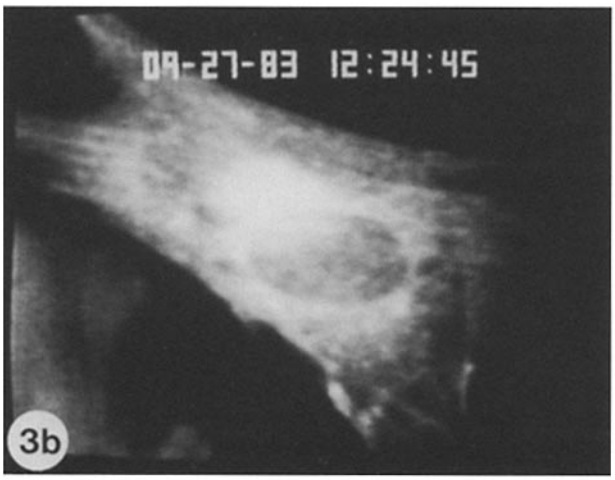

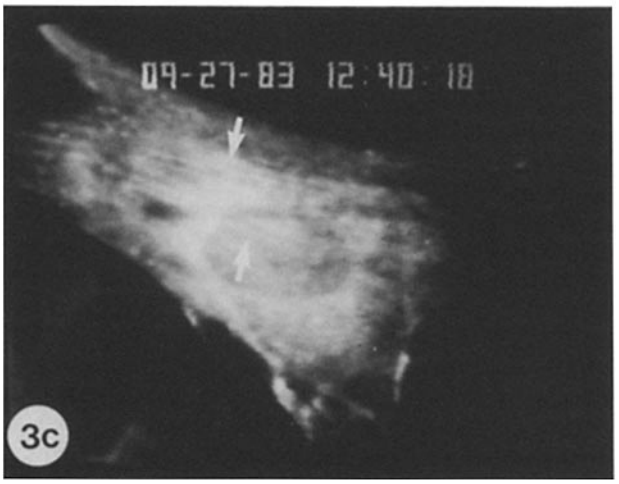

Figure 3. Sequential images of a 3T3 cell microinjected with AF-actin (*a*) 3–5 min, (*b*) 15 min, and (*c*) 30 min post-injection. Note that the actin distribution changes from nearly completely diffuse immediately after injection (*a*) to a pattern in which distinct fluorescent fibers are formed at later time points (*c*, arrows). The actin incorporates into existing stress fibers at both peripheral locations as well as in more central regions without preference. Bar, 10 μm.

one fluorescent stress fiber appeared *de novo* during this time period (28). Comparable results were obtained in four other cells analyzed in the same fashion.

FRAP. Cells were injected with AF-actin and incubated for

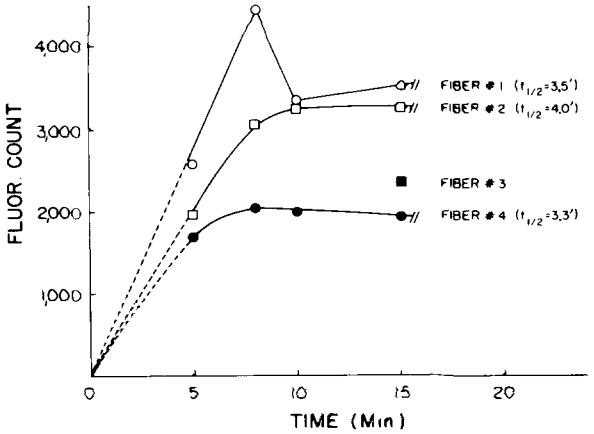

Figure 4. The rate of increase of fluorescence associated with three separate pre-existing stress fibers following the injection of AF-actin into 3T3 cells. Fiber #3 formed spontaneously during the experiment. The half-time of incorporation ranged from 3.3 to 4.0 min.

2 h to ensure complete exchange of actin subunits. Stress fibers were then bleached using a 6.0-μm radius quasi-Gaussian pattern. Recovery was monitored with full field illumination (Fig. 5). Immediately after the bleaching pulse, the bleached region could be observed (Fig. 5 *a*). Within 2 s, some recovery both in the background and in the stress fibers could be detected (Fig. 5 *b*). Extensive recovery was observed within 1 min (Fig. 5 *c*). Fig. 6 illustrates the time course of fluorescence recovery from the cell in Fig. 5. Analysis of similar data from four cells indicated that there were at least two components in the recovery process. The higher mobility component exhibited an average halftime of recovery of 37 s with a 20% immobile fraction. This corresponds to a mobility of 4.0 ($\pm$ 1.4) $\times$ 10^{-9} cm^2/s. The second component recovered very gradually over the course of several minutes and could represent recovery limited by chemical exchange of actin subunits into the stress fibers. The actin filaments in stress fibers are known to be oriented in both directions. Therefore, the lack of an obvious polarity in the recovery (Fig. 5) is not surprising. The major point to be derived from the present FRAP data is that actin subunits exchange at a high rate with actin filaments in stress fibers. Therefore, using two different types of cellular perturbations: (*a*) injection of monomers and observing incorporation, and (*b*) FRAP of equilibrated cells, we see similar results.

Cellular Polarity of Incorporation. At early time points, the fluorescent actin appears in stress fibers at peripheral locations within the cell, as well as in more central regions (Fig. 1 *a* open arrows). Thus, there appears to be no distinct cellular polarity in the association of injected actin with existing stress fibers. Furthermore, when following the incorporation of fluorescent actin into distinct structures (Figs. 3, *a–c*), fibers become increasingly fluorescent with no preferred directionality of incorporation along the length of a given fiber. It is important to emphasize that this study is concerned with the exchange of actin subunits with existing stress fibers and not the formation of new stress fibers.

Comparison of the Distributions of AF-Actin and a Control Protein. To approach the question of whether the fluorescent fibers formed by injection of AF-actin was actually due to active molecular incorporation, AF-actin was co-injected in the same cell with a heterologously labeled control protein, in

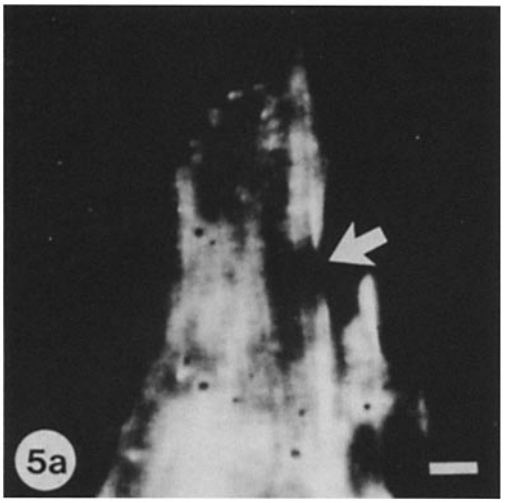

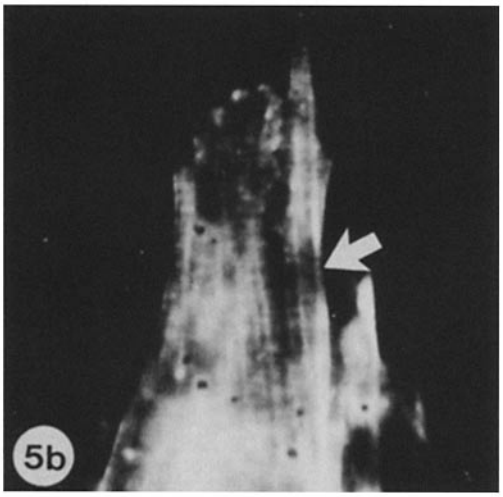

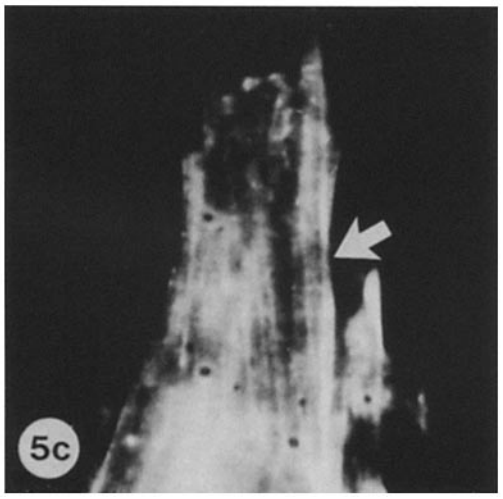

Figure 5. Living 3T3 cell, microinjected with AF-actin, 2 h post-injection. Stress fibers were photobleached with a 6.0-μm radius spot (arrow) and recovery was the monitored. (*a*) Immediately following the bleaching pulse; (*b*) 2 s after bleaching; (*c*) 1 min after bleaching. Bar, 10 μm.

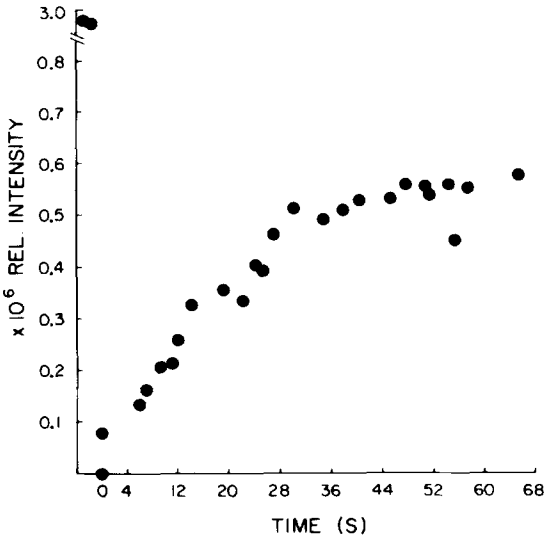

Figure 6. Plot of the recovery of fluorescence within the bleached spot depicted in Fig. 5. Image analysis of the bleached region yielded the intensity values shown. The pre-bleach intensity at time zero is shown along with the first minute of recovery. The point on the x-axis is not a data point, but marks time 0. There are at least two components of the recovery process. The higher mobility component exhibited an average halftime of recovery of 46 s with a 60% immobile fraction (3.7×10^{-9} cm^2/s). The second component recovered over several minutes and could represent recovery limited by chemical exchange of actin subunits into the stress fibers. An average of four such experiments yielded an average halftime of recovery of 37 s with a 20% immobile fraction. This corresponds to a mobility of 4.0 ($\pm$ 1.4) $\times 10^{-9}$ cm^2/s.

this case, rhodamine-labeled BSA (Fig. 7). In many cells, AF-actin formed distinct fibers (Fig. 7*b*) while the distribution of BSA was generally diffuse (Fig. 7*c*). When these cells were extracted briefly with Triton X-100 followed by fixation, resulting images of the fixed cell (Fig. 7, *d* and *e*) showed even more striking differences between the two distributions. In extracted and fixed cells, complex arrays of overlapping actin fibers were made more visible and more distinct than in the image of the living cell (Fig. 7*b*), an effect most probably due to extraction of the soluble G-actin pool and quenching of fluorescence by the fixation. Changes in the BSA images were minimal, with only a decrease in the intensity of the diffuse fluorescence noted and probably associated with both extraction and some quenching.

In other cells, however, the BSA distribution can be quite similar to the actin distribution with linear fluorescence seen in thin peripheral regions of the cell. This effect is most likely due to optical artifacts, such as pathlength of the probe and the accessible volume of the cytoplasm, perhaps due to the contours of the cell in the region of the stress fibers and/or to the volume occupied by the fiber (previously discussed in references 1, 26, and 30). A demonstration of this effect is shown in Fig. 8. The distribution of both the actin analog and the control protein are very similar in the video images of a cell fixed after co-injection (Fig. 8, *a* and *b*). Higher resolution photomicrographs of the fixed cell (Fig. 8, *c* and *d*) show that the control protein is actually excluded (arrows) from stress fibers and that linear fluorescence in the BSA image is due to pathlength artifacts and/or adventitious association of BSA with the surface of stress fibers. Therefore, actin is associated directly with the stress fibers, while BSA is excluded.

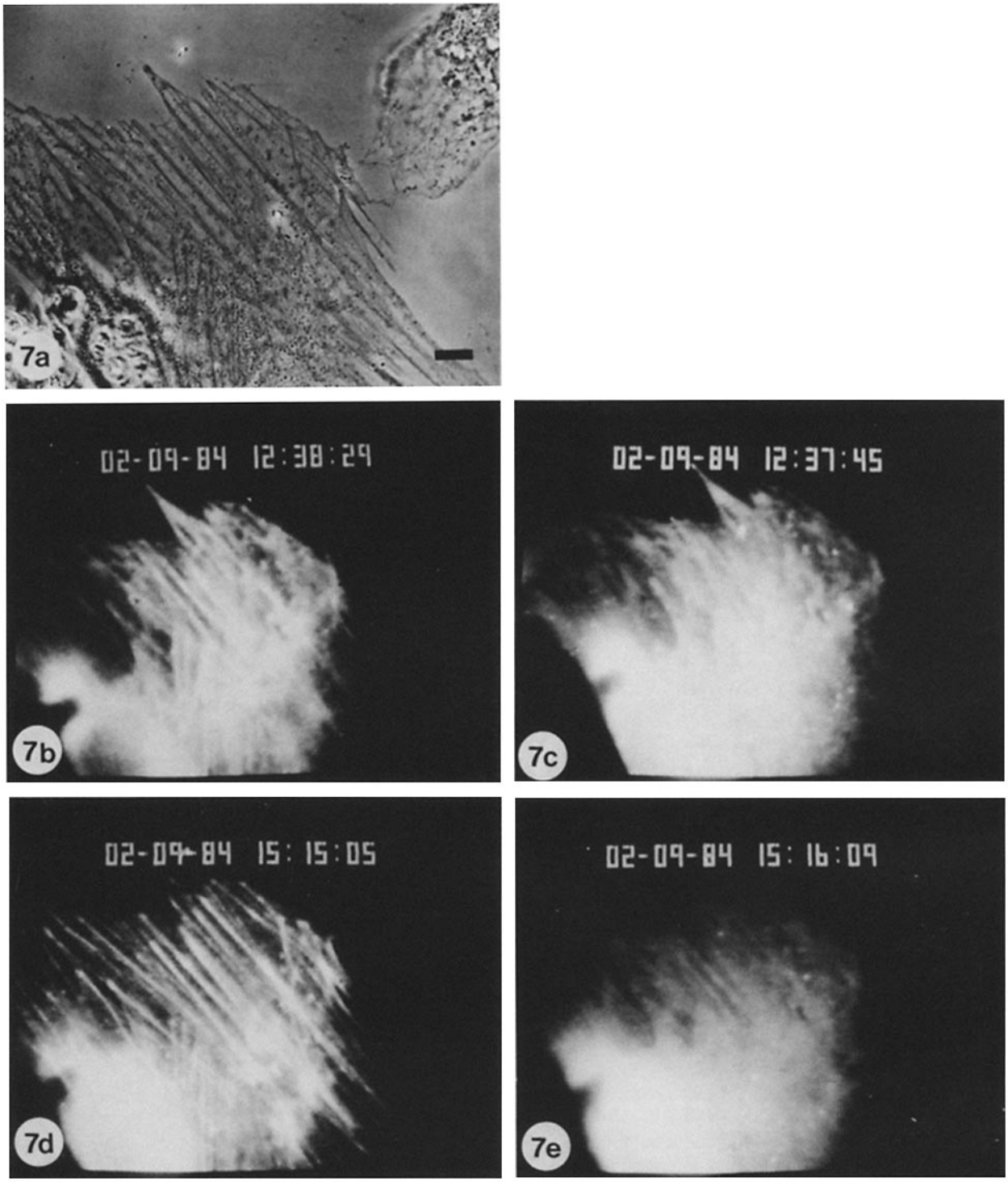

Figure 7. A 3T3 cell co-injected with AF-actin and rhodamine-labeled BSA. In the living cells, AF-actin forms distinct fibers (*b*) while the distribution of BSA is general diffuse (*c*). The same cell was extracted briefly with Triton X-100 followed by fixation. Resulting images (*d* and *e*) show even more striking differences. Complex arrays of overlapping actin fibers are made more visible (*d*) while changes in the BSA distribution (*e*) are minimal. *b–e* are video images; *a* is the same cell shown in phase contrast. Bar, 10 μm.

Molecular Incorporation of the Fluorescent Analog of Actin into Stress Fibers

Immunocytochemistry Localization of Microinjected AF-Actin. Selective immunocytochemical localization of AF-actin was performed on microinjected cells with a rabbit antibody to fluorescein (anti-fluorescein) and horseradish peroxidase coupled to goat anti-rabbit IgG. At various time periods post-injection, cells were fixed and labeled with these two antibodies and processed for immunoelectron microscopy. Thin sections were then cut parallel to the plane of the substrate.

At low magnification (Fig. 9), microinjected cells were

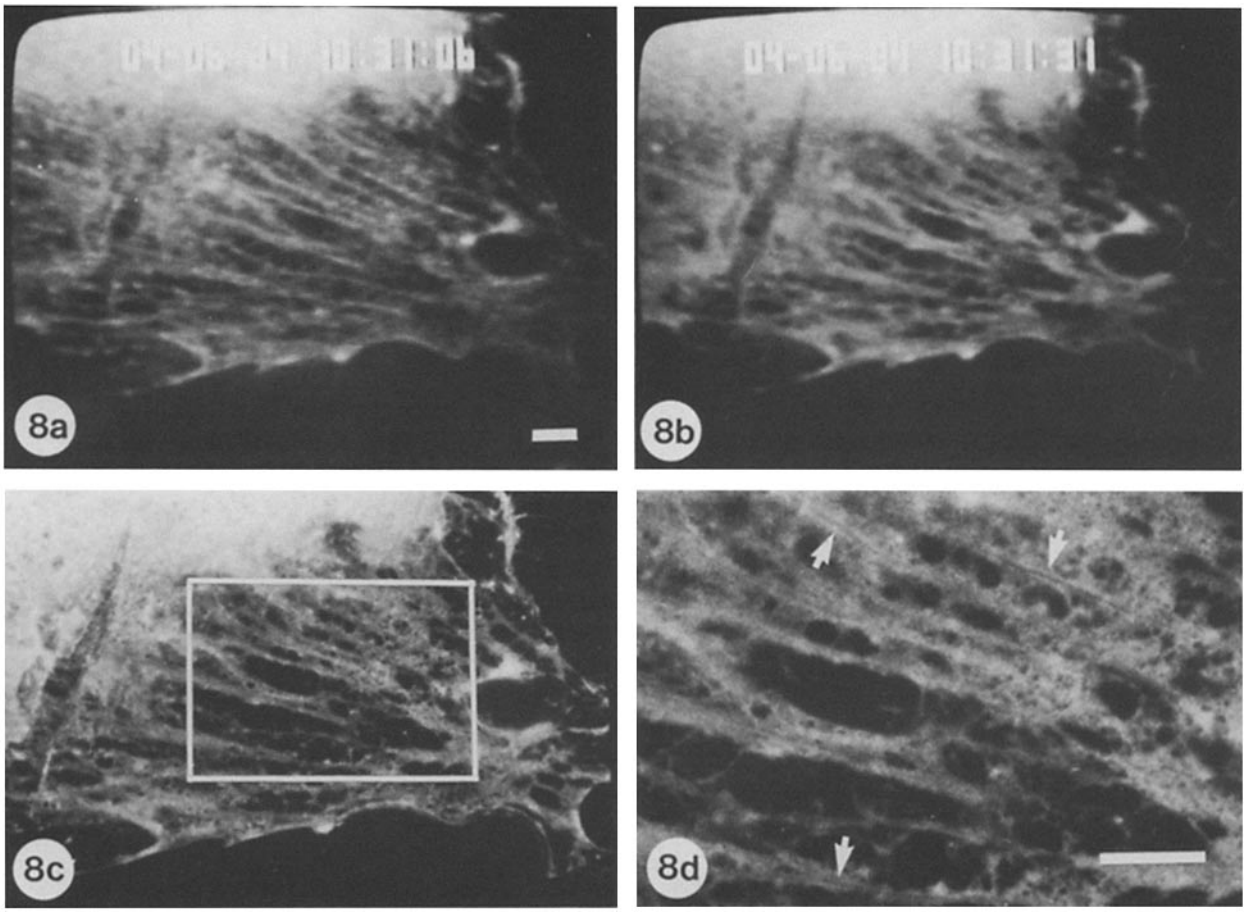

Figure 8. A 3T3 cell co-injected with AF-actin and rhodamine-labeled BSA. The distribution of both actin (*a*) and BSA (*b*) are very similar in the image intensified video images of a fixed co-injected cell. Higher resolution photomicroscopy of the same cell (*c* and *d*) show that the control protein is actually excluded from the stress fibers (arrows). *d* is the boxed area shown in *c*. Bars, (*a–c*, and *d*) 10 μm.

readily distinguishable from adjacent uninjected cells (which serve as an internal control for these experiments). Microinjected cells contained the dark reaction product within the cytoplasm. In sections closest to the substrate, differences in the juxtaposition of the cell to the substrate can be detected. Regions of the cell that are not closely apposed to the substrate are represented by interspersed electron-lucent areas.

At high magnification, several characteristics of labeled fibers were revealed. At 5 min post-injection, a periodic localization of the reaction product was sometimes seen along fibers (Fig. 10), suggesting a microheterogeneity in the incorporation of AF-actin along the length of these fiber types. This periodicity may be due to the periodic localization of actin-binding proteins, such as α-actinin, tropomyosin, and myosin, which may inhibit or stimulate actin incorporation at these sites. The periodic localization of actin at the electron microscopic level may be analogous to the punctate fluorescence seen along the length of fibers in fluorescence micrographs.

However, not all fibers exhibit distinct periodic incorporation. For example, different patterns of actin incorporation are seen in fibers of different diameters (Fig. 11). In a fiber whose diameter decreases along its length, there is an increasing density of reaction product located along the fiber as the diameter decreases (Fig. 11 *a*). It should be noted that serial sections allowed us to differentiate between real localization within the fiber bundles and surface localization. At high magnification (Fig. 11 *b*), there is non-uniform surface labeling in the wider regions of the fiber, while unlabeled thin filaments are resolvable within the core of these fibers. In an adjacent smaller diameter fiber, more extensive labeling occurred during the same time period and thin filaments within the core were obscured by the reaction product. It is likely that not all stress fibers have the same protein composition and that some stress fibers may be in different stages of formation or dissolution. Therefore, multiple patterns of actin subunit association and/or exchange is not unexpected.

By 20 min post-injection (Fig. 12), most fibers were labeled uniformly throughout, regardless of diameter, suggesting that complete incorporation of actin throughout fibers occurred in this time period. These results are consistent with both the rate of incorporation data (Fig. 4) and the FRAP data (Fig. 5 and 6).

Control cells (uninjected cells exposed to both primary and secondary antibodies) contain fibers which never showed any evidence of reaction product and in which individual actin filaments were clearly resolvable at high magnification (Fig. 13).

Templating of Endogenous Stress Fibers in Cell Models with the Fluorescent Analog of Actin. A cell model was prepared in which fixed stress fibers were incubated with filamentous AF-actin under conditions in which no exchange

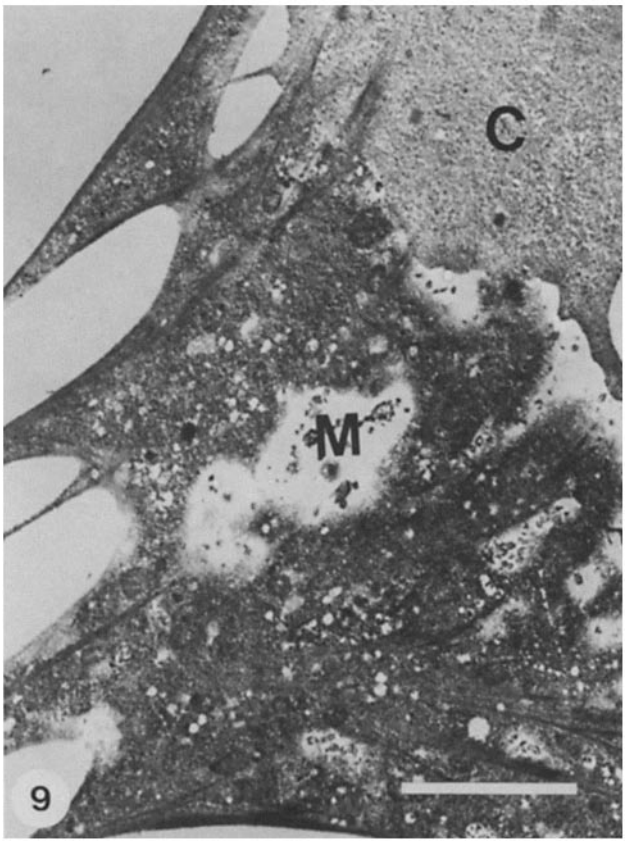

Figure 9. Electron micrograph of a microinjected cell labeled with anti-fluorescein and peroxidase-coupled IgG. At low magnification, the microinjected cell (*M*) is readily distinguishable from an adjacent uninjected cell (*C*) by the dark reaction product within the cytoplasm. Regions of the cell that are not closely opposed to the substrate are represented by interspersed electron-lucent areas. Bar, 5.0 μm.

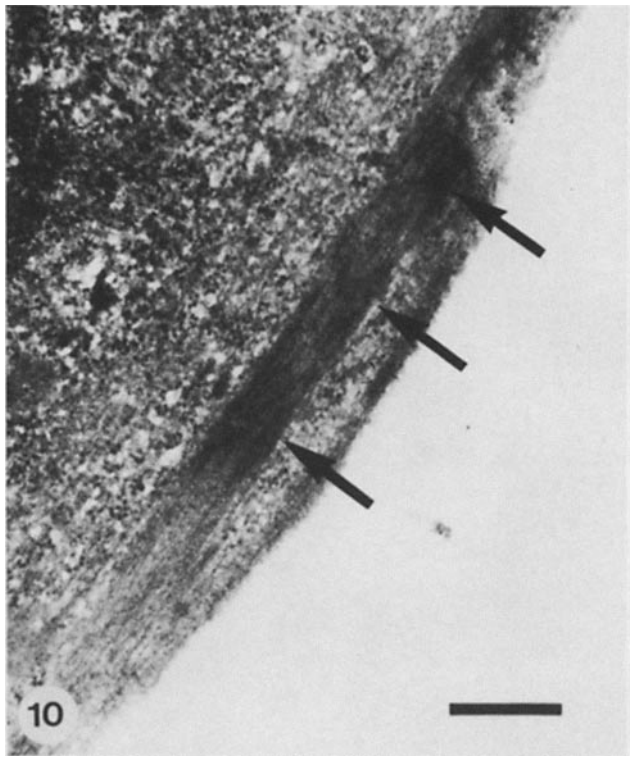

Figure 10. A microinjected cell fixed at 5 min post-injection and labeled with anti-fluorescein and peroxidase-coupled IgG. A periodic localization of the reaction product is seen along the length of some fibers (arrows). Bar, 0.5 μm.

or incorporation of AF-actin was possible, a process we call "templating" (see Materials and Methods). After templating, cells were labeled with anti-fluorescein followed by either rhodamine- or peroxidase-labeled IgG (Fig. 14). Fluorescence microscopy revealed that templated stress fibers were not too different in appearance than living microinjected cells. However, electron microscopy revealed that such fibers never showed uniform reaction product throughout the fibers. In fact, a non-uniform distribution of reaction product along the length of the fiber was detected, with bare zones in some areas in which filaments were resolved (Fig. 14*a*). Therefore the uniform distribution of reaction product throughout the diameter of stress fibers in microinjected cells (Fig. 12) lends support for molecular incorporation of the analog throughout the filaments of the fiber, as opposed to a nonspecific adherence of the analog to the surfaces of existing stress fibers.

Discussion

In this study, we present evidence that the fluorescent analog of actin exchanges rapidly with endogenous actin subunits in filaments within stress fibers at the molecular level. Fluorescently labeled actin, microinjected in the G-form, was incorporated into distinct fluorescent fibers as early as 5 min post-injection. This finding is in agreement with those of Glacy (4) for the incorporation of rhodamine-labeled actin into fibers of chick fibroblasts. In our study, actin was incorporated or exchanged in both peripheral and perinuclear regions without preference. In addition, fibers that were centrally located exhibited exchange of actin subunits along the whole length of the fibers. FRAP studies supported the incorporation experiments indicating that soluble actin subunits could exchange rapidly with actin subunits in filaments of stress fibers. Further FRAP studies on actin arrays with known polarities could now be used to test for the treadmill model of actin assembly in vivo.

Wang (28) has reported that for fibers forming near the leading and trailing ends of cells, actin becomes incorporated first as discrete spots and then unidirectionally into extended fibers. While this latter study described the *de novo* formation of stress fibers, we have studied the exchange of subunits within existing fibers. It must be emphasized that multiple mechanisms of subunit exchange and stress fiber formation may exist due to the heterogeneity of protein compositions of stress fibers. For example, Lin et al. (15) have isolated two classes of microfilaments from the same cell type, tropomyosin-enriched and α-actinin-enriched microfilaments. Furthermore, differences in stress fiber composition have also been reported for different cell types (21).

We have used immunoelectron microscopy to increase the resolution for determining the mode of association of the actin analog with stress fibers. For these studies, the analog was localized at various time points after injection using an anti-fluorescein antibody and a secondary antibody coupled to horseradish perioxidase. At 5 min post-injection, the analog is localized mainly on the surface of fibers with unincorpor-

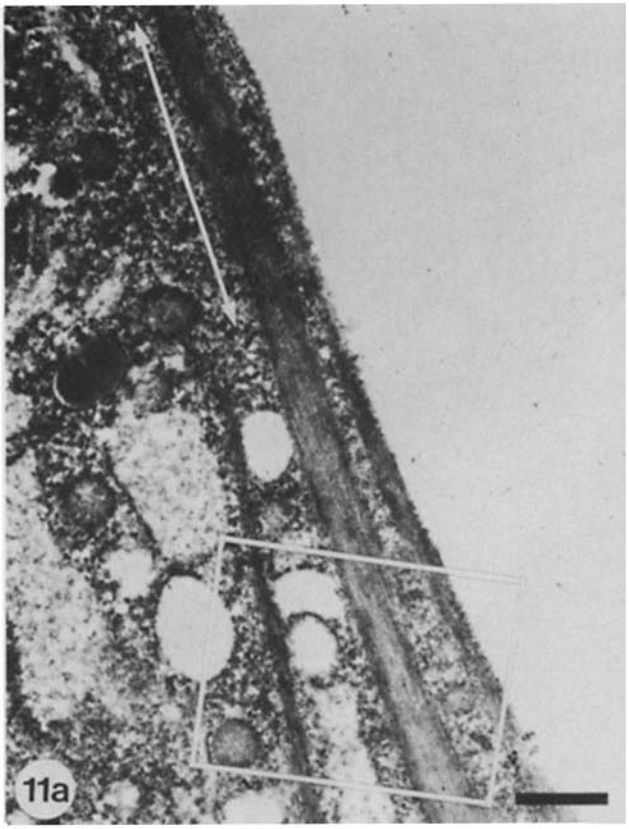

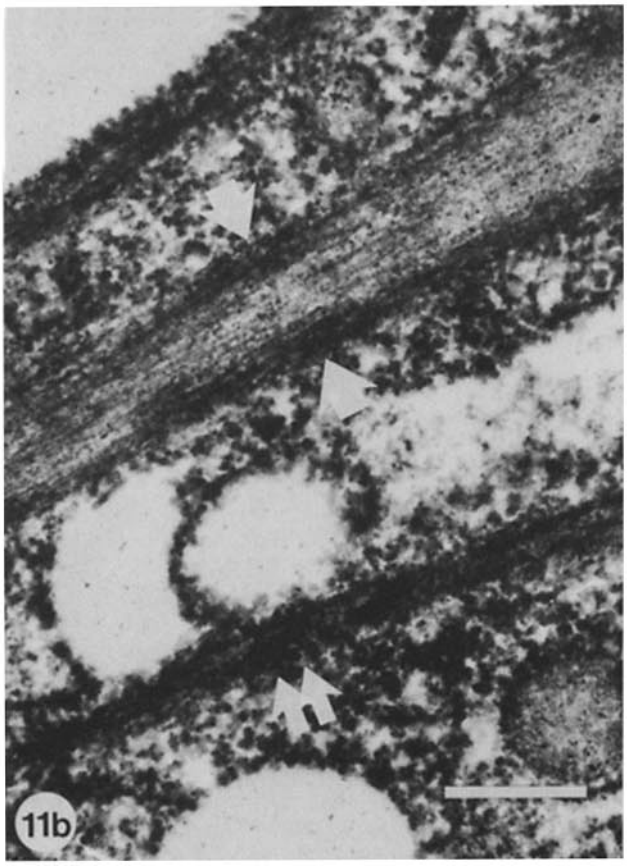

Figure 11. A microinjected cell fixed at 5 min post-injection and labeled with anti-fluorescein and peroxidase-coupled IgG. In a fiber whose diameter decreases along its length, there is an increasing amount of reaction product as the diameter decreases (*a*, delineated by arrows). Note the non-uniform surface labeling in wider regions of the fiber (*b*, arrows). In an adjacent smaller diameter fiber, labeling occurs throughout its diameter (*b*, double arrows). *b* is the boxed area shown in *a*. Bars (*a*) 1.0 μm; (*b*) 0.5 μm.

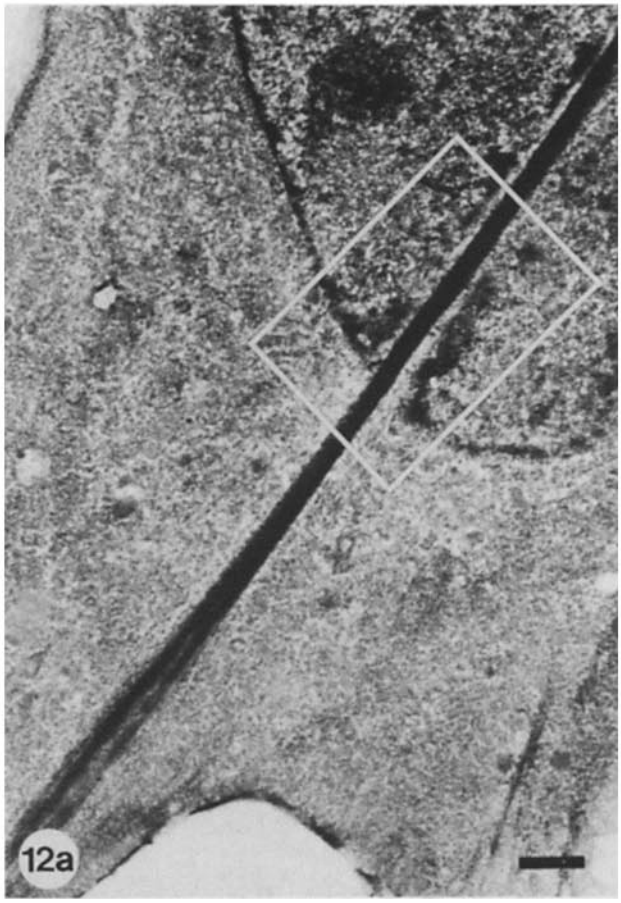

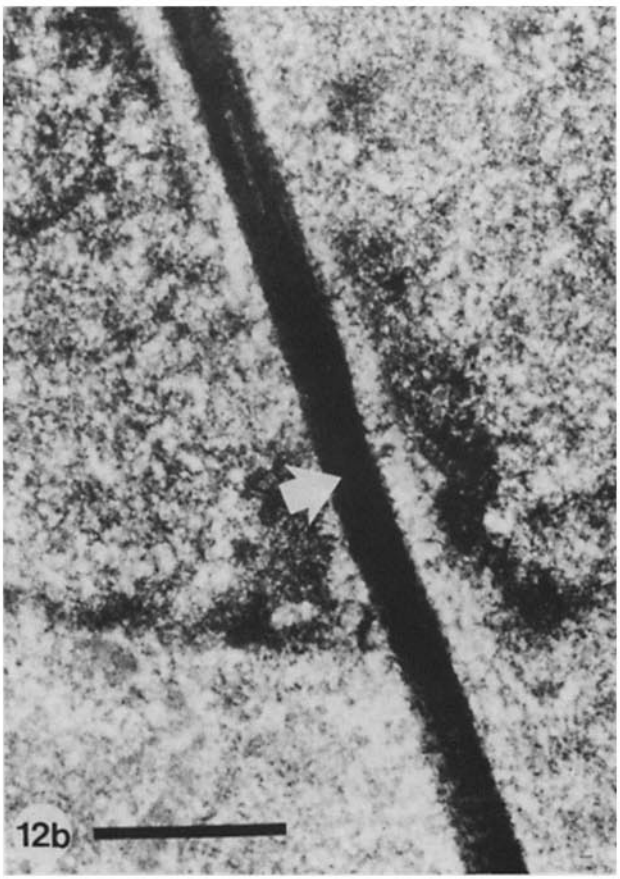

Figure 12. A microinjected cell fixed at 20 min post-injection and labeled with anti-fluorescein and peroxidase-coupled IgG. Most fibers are labeled uniformly throughout (*b*, arrow), regardless of diameter. *b* is the boxed area shown in *a*. Bars, 1.0 μm.

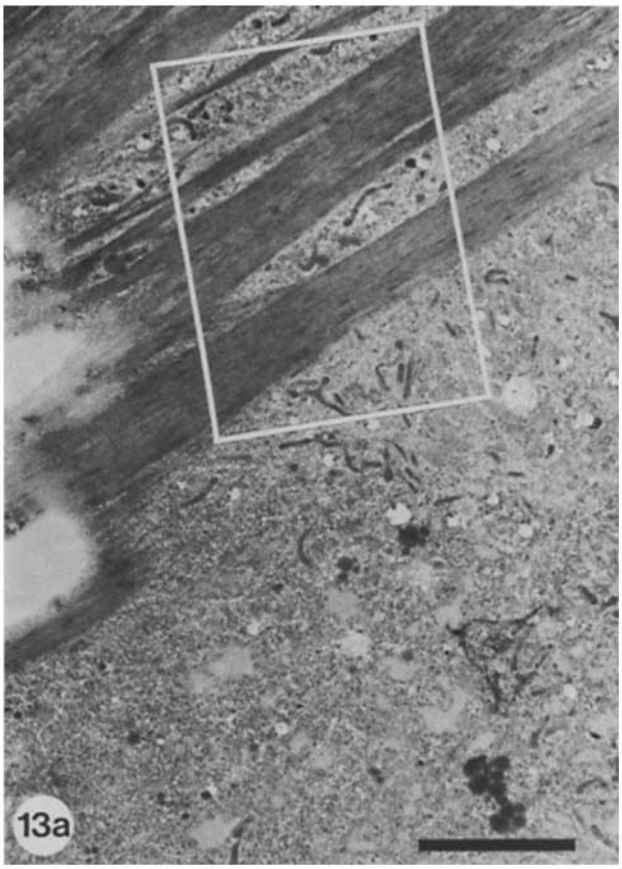

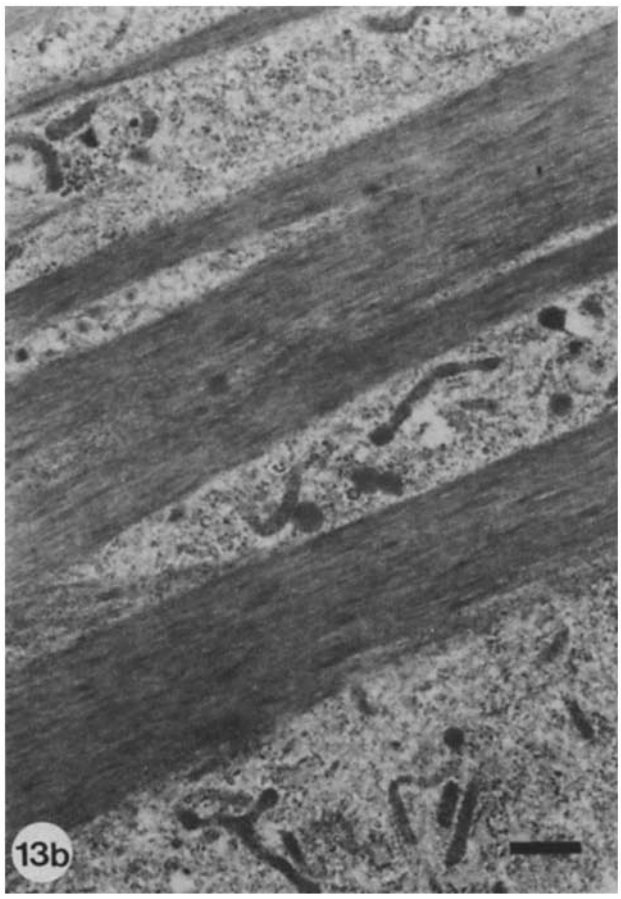

Figure 13. Control cells (uninjected cells exposed to both primary and secondary antibodies). Fibers never showed any evidence of reaction product. Individual actin filaments are clearly resolvable at high magnification. *b* is the boxed area shown in *a*. Bars, (*a*) 5.0 μm; (*b*) 1.0 μm.

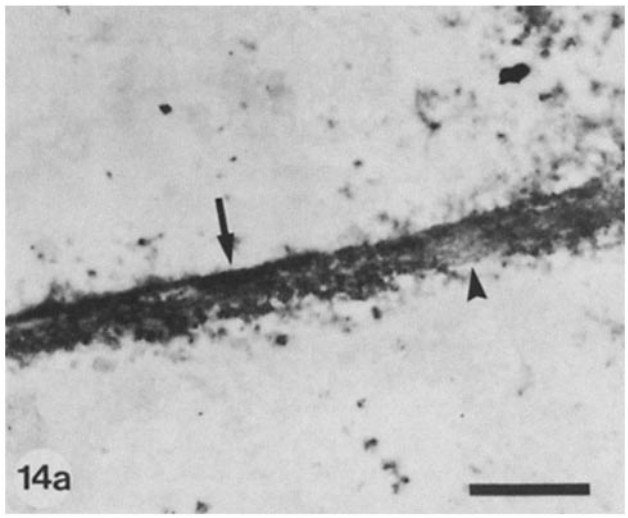

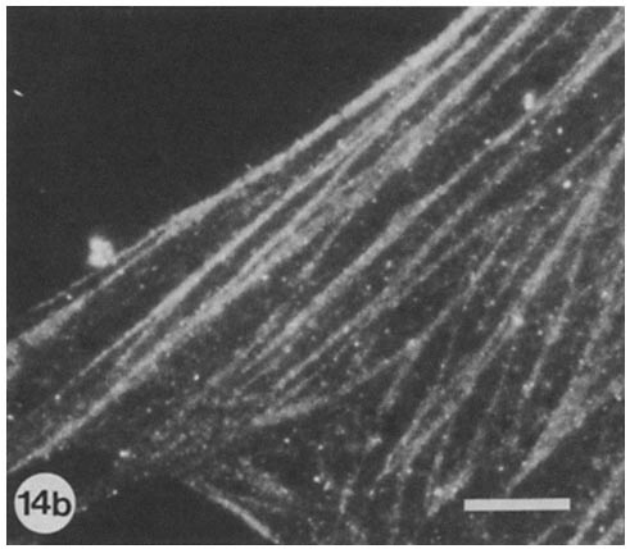

Figure 14. Cell models templated with AF-actin, labeled with anti-fluorescein, followed by peroxidase-labeled IgG (*a*) or rhodamine-labeled IgG (*b*). Stress fibers are non-uniformly fluorescent with bright foci located in the background as well as on fibers (*b*). Stress fibers show an uneven distribution of reaction product (*a*, arrow) with bare zones containing filaments visible in some regions (*a*, arrowhead). Bars, (*a*) 1.0 μm; (*b*) 10 μm.

ated, individual filaments resolvable within the core of the fiber. In some cells, the reaction product extends into the core of the fiber at sites located periodically along the length of the fiber. We propose that after microinjection, AF-actin is first incorporated into filaments at numerous sites (i.e., ends of filaments) along the surface of fibers, and then into more centrally located filaments. The existence of an array or matrix of actin-binding proteins at discrete periodic locations along the length may either inhibit or promote the incorporation at these sites. This may occur, for example, if certain actin-binding proteins act as capping proteins which inhibit the turnover of actin at the ends of filaments. After a steady state has been reached, actin is incorporated uniformly throughout all the filaments within a fiber.

Summary and Prospectus

The results of this study have convinced us that a fluorescent analog of actin can incorporate into actin filaments within stress fibers at the molecular level. The rate of actin subunit exchange suggests that stress fibers are not static structures but are highly dynamic organelles.

The results obtained with a single fluorescent analog must be compared to those in which the site of modification and the fluorophore bound to the analog have been changed. This approach will optimize the ability to obtain physiologically relevant information using this technique. It is expected that some analog functions will be reduced compared to the native molecule. Therefore, different analogs of the same protein will be required. For example, it has been reported that actin modified at Cys-374 has a reduced interaction with profilin when assayed in vitro (17a). Whether this has any effect in the living cell is not yet clear. However, it must be pointed out that the time course of the recovery after photobleaching of stress fibers was similar for Cys-374 modified actin and for a lysine modified actin (10). A comparison of the dynamics of two different fluorescent analogs is currently under investigation.

At least with actin, the use of fluorescent analog cytochemistry can be extended and used to its fullest advantage by performing quantitative studies using FRAP, fluorescence anisotropy, resonance energy transfer, total internal reflection fluorescence, and a variety of other spectroscopic methods (23). The availability of low light level cameras, in combination with digital image processing techniques, will permit image acquisition at ultra-low light levels and subsequent image analysis procedures can quantify results. Used concurrently, these techniques will allow the temporal and spatial dynamics of selected molecular processes to be determined in living cells during actual cellular events (23–25, 29) and should have a major impact on several areas of cell biology.

The authors would like to gratefully acknowledge the collaboration and assistance of Drs. Katherine Luby-Phelps and Frederick Lanni in the FRAP experiments. The authors would also like to thank Dr. Katherine Luby-Phelps for the gift of the anti-fluorescein antibody, along with Dr. Paul McNeil, for reviewing the manuscript, and Ms. Bonnie Chojnacki for her excellent technical assistance.

This work was supported by grants from The Council for Tobacco Research-U.S.A. (#1412R2) and the National Institutes of Health (AM32461).

Received for publication 25 March 1985, and in revised form 1 October 1985.

References

1. Amato, P. A., E. R. Unanue, and D. L. Taylor. 1983. Distribution of actin in spreading macrophages: a comparative study on living and fixed cells. *J. Cell Biol.* 96:750–761.

2. Buckley, I. K., and K. R. Porter. 1967. Cytoplasmic fibrils in living cultured cells: a light and electron microscope study. *Protoplasma.* 64:349–380.

3. Fujiwara, K., and T. D. Pollard. 1976. Fluorescent antibody localization of myosin in the cytoplasm, cleavage, furow, and mitotic spindle of human cells. *J. Cell Biol.* 71:848–875.

4. Glacy, S. D. 1983. Subcellular distribution of rhodamine-actin microinjected into living fibroblastic cells. *J. Cell Biol.* 97:1207–1213.

5. Goldman, R. D., E. Lazarides, R. Pollack, and K. Weber. 1975. The distribution of actin in non-muscle cells: the use of actin antibody in the localization of actin within the microfilament bundles of mouse 3T3 cells. *Exp. Cell Res.* 90:333–344.

6. Gordon, W. E. 1978. Immunofluorescent and ultrastructural studies of "sarcomeric" units in stress fibers of cultured non-muscle cells. *Exp. Cell Res.* 117:253–250.

7. Isenberg, G., P. C. Rathke, N. Hulsmann, W. W. Franke, and K. E. Wohlfarth-Bottermann. 1976. Cytoplasmic actomyosin fibrils in tissue culture cells: direct proof of contractability by visualization of ATP-induced contraction in fibrils isolated by laser microbeam dissection. *Cell Tissue Res.* 166:427–443.

8. Kreis, T. E., and W. Birchmeier. 1980. Stress fiber sarcomeres of fibroblasts are contractile. *Cell.* 22:555–561.

9. Kreis, T. E., K. H. Winterhalter, and H. Birchmeier. 1979. In vivo distribution and turnover of fluorescently labeled actin microinjected into human fibroblasts. *Proc. Natl. Acad. Sci. USA.* 76:3814–3818.

10. Kreis, T. E., B. Geiger, and J. Schlessinger. 1982. Mobility of microinjected rhodamine actin within living chicken gizzard cells determined by fluorescence photobleaching recovery. *Cell.* 29:835–845.

11. Langanger, G., J. De Mey, M. Moeremans, G. Daneels, M. De Brabander, and J. V. Small. 1984. Ultrastructural localization of α-actinin and filamin in cultured cells with the immunogold staining (IGS) method. *J. Cell Biol.* 99:1324–1334.

12. Lazarides, E. 1975. Tropomyosin antibody: the specific localization of tropomyosin in non-muscle cells. *J. Cell Biol.* 65:549–561.

13. Lazarides, E., and K. Burridge. 1975. Alpha-actinin: immunofluorescent localization of a muscle structural protein in nonmuscle cells. *Cell.* 6:289–298.

14. Lazarides, E., and K. Weber. 1974. Actin antibody: the specific visualization of actin filaments in non-muscle cells. *Proc. Natl. Acad. Sci. USA.* 71:2268–2272.

15. Lin, J. J.-C., F. Matsumura, and S. Yamashiro-Matsumura. 1984. Tropomyosin-enriched and alpha-actinin–enriched microfilaments isolated from chicken embryo fibroblasts by monoclonal antibodies. *J. Cell Biol.* 98:116–127.

16. Luby-Phelps, K., P. A. Amato, and D. L. Taylor. 1984. Selective immunocytochemical detection of fluorescent analogs with antibodies specific for the fluorophore. *Cell Motility.* 4:137–149.

17. Luby-Phelps, K., F. Lanni, and D. L. Taylor. 1985. Behavior of a fluorescent analogue of calmodulin in living 3T3 cells. *J. Cell Biol.* 101:1245–1256.

17a.Malm, B. 1984. Chemical modification of Cys-374 of actin interferes with the formation of the profilactin complex. *FEBS (Fed. Eur. Biochem. Soc.) Lett.* 173:399–402.

18. Sanger, J. W. 1975. Intracellular localization of actin with fluorescently labelled heavy meromyosin. *Cell Tissue Res.* 161:432–444.

19. Sanger, J. W., B. Mittal, and J. M. Sanger. 1984. Interaction of fluorescently labeled contractile proteins with the cytoskeleton in cell models. *J. Cell Biol.* 99:918–928.

20. Sanger, J. M., and J. W. Sanger. 1980. Banding and polarity of actin filaments in interphase and cleaving cells. *J. Cell Biol.* 86:568–575.

21. Sanger, J. W., J. M. Sanger, and B. M. Jackusch. 1983. Differences in the stress fibers between fibroblasts and epithelial cells. *J. Cell Biol.* 96:961–969.

22. Schloss, J. A., and R. D. Goldman. 1979. Isolation of a high molecular weight actin-binding protein from baby hamster kidney (BHK-21) cells. *Proc. Natl. Acad. Sci. USA.* 76:4484–4488.

23. Taylor, D. L., P. A. Amato, K. Luby-Phelps, and P. McNeil. 1984. Fluorescent analog cytochemistry. *Trends Biochem. Sci.* 9:88–91.

24. Taylor, D. L., P. A. Amato, F. Lanni, P. McNeil, K. Luby-Phelps, and L. Tanasugarn. 1985. The dynamics of specific molecules and ions in living cells. *In* Proceedings of the Yamada Conference on Cell Motility. University of Tokyo Press. In press.

25. Taylor, D. L., and Y.-L. Wang. 1980. Fluorescently labeled molecules as probes of the structure and function of living cells. *Nature (Lond.).* 284:405–410.

26. Taylor, D. L., Y.-L. Wang, and J. M. Heiple. 1980. Contractile basis of ameboid movement. VII. The distribution of fluorescently labeled actin in living amebas. *J. Cell Biol.* 86:590–598.

27. Wang, K., J. F. Ash, and S. J. Singer. 1975. Filamin, a new high-molecular-weight protein found in smooth muscle and non-muscle cells. *Proc. Natl. Acad. Sci. USA.* 72:4483–4486.

28. Wang, Y.-L. 1984. Reorganization of actin filament bundles in living fibroblasts. *J. Cell Biol.* 99:1478–1485.

29. Wang, Y.-L., J. M. Heiple, and D. L. Taylor. 1981. Fluorescent analog cytochemistry of contractile proteins. *Methods Cell Biol.* 25(Pt. B):1–11.

30. Wang, Y.-L., and D. L. Taylor. 1979. Distribution of fluorescently labeled actin in living sea urchin eggs during early development. *J. Cell Biol.* 82:672–679.

31. Wang, Y.-L., and D. L. Taylor. 1980. Preparation and characterization of a new molecular cytochemical probe: 5-iodoacetamide fluorescein-labeled actin. *J. Histochem. Cytochem.* 28:1198–1206.

32. Weber, K., and U. Groeschel-Stewart. 1974. Antibody to myosin: the specific visualization of myosin containing filaments in non-muscle cells. *Proc. Natl. Acad. Sci. USA.* 71:4561–4564.

33. Wehland, J., and K. Weber. 1980. Distribution of fluorescently labeled actin and tropomyosin after microinjection in living tissue culture cells observed with TV image intensification. *Exp. Cell Res.* 127:397–408.